Effect of nucleating agents and iron oxide content on the structure and the magnetic properties of magnetite-based glass-ceramics

E. Cimpoiasu[*], V. Sandu[**], A. Kuncser[**, ***], M.S. Nicolescu[**]

[*]U.S. Naval Academy, Physics Dept., Annapolis, MD, USA
[**]National Institute of Materials Physics, Bucharest Magurele, 077125, Romania
[***]Bucharest University, Faculty of Physics 077125, Bucharest-Magurele, Romania

ABSTRACT

Magnetite nanoentities were grown in a glassy matrix by controlled crystallization of Fe-containing borosilicate and boroaluminosilicate glasses. Their structure, morphopology and magnetic blocking temperatures were investigated with regard to the effect of the nucleating agents and the content of iron oxides.

Keywords: magnetite, glass ceramics, magnetization, superparamagnetism, nucleating agent.

1 INTRODUCTION

Glass-ceramics with magnetic properties are a class of materials consisting of a glassy matrix in which a magnetic phase crystallizes. They are obtained by controlled crystallization of a parent glass which contains magnetic ions. The interest in using borosilicate glasses as a precursor for glass-ceramics stems from the tendency of these glasses toward phase separation. This separation is generated by the tendency of the glass former ions (Si^{4+}, B^{3+}, Fe^{3+}, and Al^{3+}) to occupy preferred sites or coordination numbers. The addition of glass modifiers expands the fabrication flexibility of the glass-ceramics [1,2] by controlling the conversion from trigonal [BO_3] to tetrahedral [BO_4] coordination in silica base glass. In addition to the oxidic ingredients used for the fabrication of the parent glass, the nature of the nucleating agents seems to be highly relevant to the magnetic properties of the resulting glass-ceramics as well because they facilitate/ inhibit the formation of certain phases and impose a specific growth pattern.

In this paper, we present the effect of using two nucleating agents, namely, P_2O_5 and Cr_2O_3, to obtain magnetic glass-ceramics from Fe containing borosilicate parent glasses. The choice is based on the different mechanisms involved in the process of nuclei formation generated by the two oxides. Moreover, we used two different iron oxide contents as well, in order to explore the effect of iron-rich conditions on the glass formations. In this report we compare and contrast results for these four categories of sample regarding the structure, morphology and the magnetic properties, as revealed by the magnetic blocking temperatures distribution.

2 MATERIALS AND METHODS

Magnetite-based glass-ceramics were fabricated starting from borosilicate glasses with a constant content of boron and sodium, but different content of iron oxides and different nucleating agents, namely Cr_2O_3 (BSFC17 and BSFC24) and P_2O_5 (BSFP17 and BSFP24). The composition of the batches is given in the Table I.

Sample	Composition(wt%)						
	SiO_2	B_2O_3	Na_2O	Fe_2O_3	Al_2O_3	Cr_2O_3	P_2O_5
BSFC17	43.5	28.6	6.4	17.5	3.5	0.5	0
BSFP17	46.5	28.6	6.4	17.5	0	0	1.0
BSFC24	36.5	28.6	6.4	24.5	3.5	0.5	0
BSFP24	39.5	28.6	6.4	24.5	0	0	1.0

Table 1: Batch composition of the parent glasses.

All the ingredients mentioned above were mixed together and the blends were heated in alumina crucibles in contact with air. More details about the parameters of the melting and crystallization processes can be found elsewhere [3].

High resolution micrographs were obtained with an analytical transmission electron microscope JEM-ARM200F. The magnetic properties were investigated with a MPMS SQUID magnetometer (Quantum Design) in the temperature range 5-300 K and magnetic fields up to 2 T.

3 RESULTS AND DISCUSSIONS

3.1 Phase Structure

The XRD data analysis of these samples showed that the crystalline phase in the bulk is magnetite in all samples [4,5]. Mössbauer data also confirms the presence of magnetite as unique phase in all bulk samples [4].

In all categories of samples, the microscopy data show the presence of magnetic entities that exhibit a complex size distribution. This can be seen in the HRTEM micrographs shown in the insets to Figs. 1 and 2. Specifically, there are mainly two categories of entities. On one hand, there is a series of submicron multicore magnetite crystallites up to 100 nm in size in the lower-iron samples and 200 nm in the iron-rich samples. These large crystallites provide those

features typical for magnetite like Verwey and Curie temperatures. The multicore crystallites, as most obviously observed in the iron-rich samples, are built of relatively large and well-defined nanoparticles (size up to 50 nm).

On the other hand, there is a collection of small nanoparticles of smaller size, below ~30 nm which lead to a superparamagnetic behavior. These smaller crystallites, which are also magnetite, have a complex distribution of the grain size. Specifically, except for the sample BSFC17, they show a bimodal distribution of the grain size, and the bimodalism is emphasized in the samples with P_2O_5 as nucleating agent. The main panels of the Figs. 1 and 2 show the size distributions of the magnetite nanoparticles and the fits of these distribution with one or two lognormal distribution functions. The medians for the modes, as extracted from fits, are:

i) BSFC17 has one single noticeable peak at d_{md} = 9.8 ±0.5 nm;

ii) BSFP17, d_{md} = 5.4±0.1 nm for the small nanoparticles and d_{md} = 21.2 ±0.5 nm for the high size mode;

iii) BSFC24, d_{md} = 7.2±2.8 nm for the small nanoparticles and d_{md} = 22.7 ±1.0 nm for the larger ones;

iv) BSFP24, d_{md} = 4.7 ± 0.2 for the small size mode and d_{md} = 15.2 ± 0.4 nm for the larger nanoparticles.

From the structure and microscopy results, the effect of the nucleation agent is easy to point out. Independent of the iron content, P_2O_5 induces a well-separated bimodal distribution of nanoparticle sizes, consisting of very small nanoparticles of ~ 5 nm in diameter, and larger ones of ~ 20 nm in diameter. Interestingly enough, the larger the content of iron, the smaller are the median sizes of the nanoparticles (4.7 nm vs. 5.4 nm, and 15.2 nm vs. 21.2 nm).

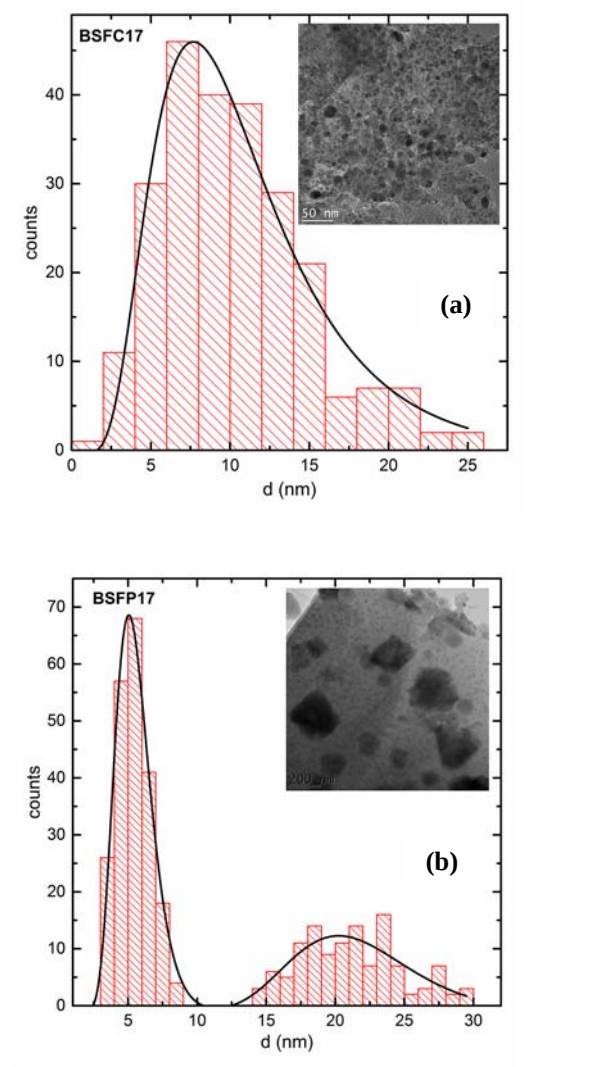

Figure 1: HRTEM micrographs (inset) and the associated size distribution of the small nanoclusters (main panel) for (a) BSFC17 and (b) BSFP17.

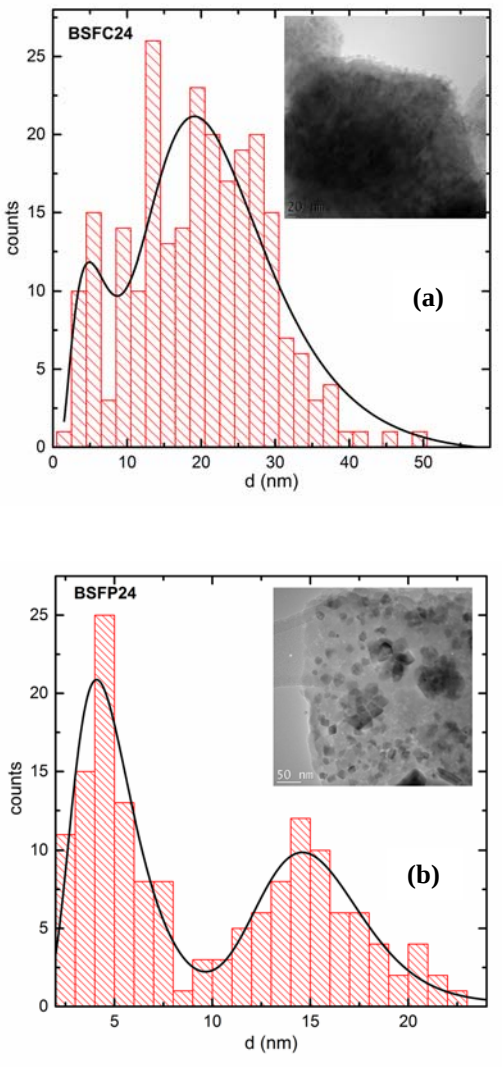

Figure 2: HRTEM micrographs (inset) and the associated size distribution of the small nanoclusters (main panel) for (a) BSFC24 and (b) BSFP24.

The case of Cr_2O_5 is different. In the case of the lower-iron content sample BSFC17, a clear bimodal distribution is harder to single out using fits. The distribution is wide, with a dominant size at about 8-10 nm and possibly a very small peak at about 20 nm. Fits for the iron-rich sample BSFC24 indicate a large peak at about 21 nm, and a small and narrow peak at 5 nm. Thus, in the case of Cr_2O_5 nucleating agent, larger amount of iron results in larger nanoparticles (21 nm vs 10 nm), in contradiction to the effect of the P_2O_5.

3.2 Distribution of the blocking temperatures

In the case of free magnetic nanoparticles, the relaxation of any magnetic configuration is controlled by the anisotropy energy barrier of density K_{eff}. Thus, for activated processes at a given temperature T, the relaxation time τ for a monodisperse system of particles of volume V is given by [5]:

$$\tau = \tau_0 \exp(K_{eff} V / k_B T) \quad (1)$$

where τ_0 is an attempt relaxation time. If the temperature is high enough, the relaxation time reaches the order of the measurement time τ_m. The corresponding temperature is known as blocking temperature T_B, i.e., $\tau(T_B) = \tau_m$. Thus, below T_B, any measurement of characteristic time τ_m perceives the system as blocked in a certain magnetic state.

Our glass-ceramics have a complex structure with multicore submicron particles, bimodally distributed nanoparticles and a glassy matrix with paramagnetic properties generated by the Fe ions remaining in the glass network. Because the size distribution is polydisperse, an average T_B cannot be defined and, at a given T, there is a mixture of blocked and unblocked nanoparticles. Consequently, it is better to define a distribution function of the blocking temperatures $f(T_B)$ which depicts in detail the unblocking process of the macrospins and should, in large terms, correlate to the size distribution functions. The distribution function $f(T_B)$ can be obtained from dc-magnetization as the temperature derivative of the zero field-cooled and field-cooled magnetization, m_{ZFC} and m_{FC}, respectively [5]:

$$f(T_B) \sim \frac{d(m_{ZFC} - m_{FC})}{dT} \quad (2)$$

Figs. 3 and 4 show the distribution of the blocking temperatures for all the four categories of samples determined from the magnetization data, as described above. All the distributions display few common characteristics, like a largest peak that happens at T_{BM}, a shoulder peak that happens at T_S, and a small peak (unmarked on the pictures) that happens at about 120 K.

There are though clear differences as well. First of all, starting with the P_2O_5-based samples, both peaks T_{BM} and T_S

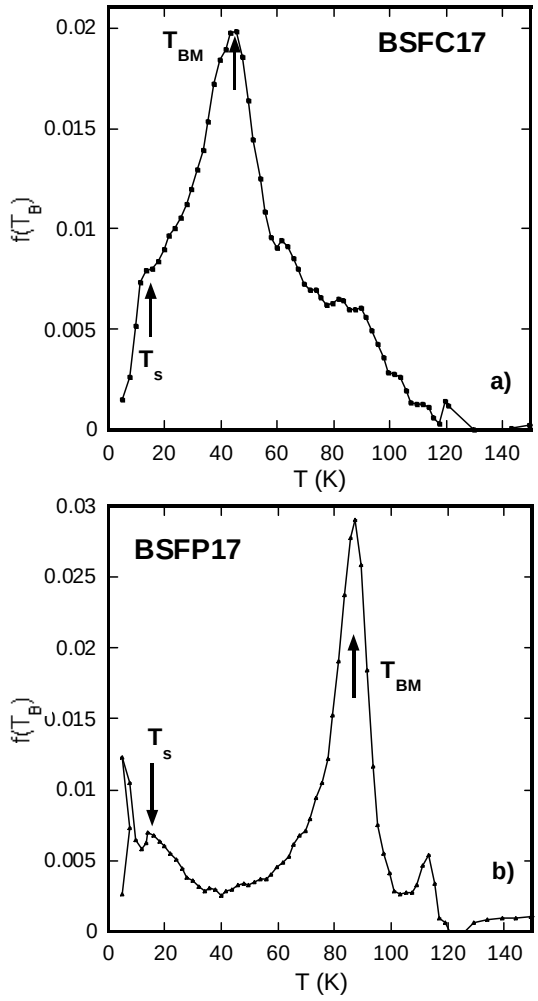

Figure 3: Temperature dependence of the distribution function $f(T_B)$ for (a) BSFC17 and (b) BSFP17.

are shifted towards higher temperatures for the iron-rich sample BSFP24 by 21 K (109 K vs 88 K, and 37 K vs 14 K) compared to the peaks of BSFP17. Despite this shift, the "bimodal" distribution is present in both samples, in accordance to the structural size distribution. The shift towards higher temperatures suggests maybe contributions from interparticle interaction, larger in the case of BSFP24 compared to BSFP17, as confirmed by Ref. 5.

The case of the Cr_2O_5-based samples, BSFC17 and BSFC24, is more complex. The shoulder peak for both samples happens at T_S = 12 K, at approximately the same T_S value of the iron-rich BSFP17. The largest peak of the distributions happens at different temperatures, though. Specifically, for BSFC17, T_{BM} = 43 K. For BSFC24, the 43 K peak is present as well (labeled here T_{BM}'), but it is weaker than the dominat one which happens at T_{BM} = 98 K. If we refer back to the size distribution in BSFC24 vs BSFC17, and the observation that iron-rich environment for the Cr_2O_5 nucleating agent resulted in more 20 nm-sized particles, one

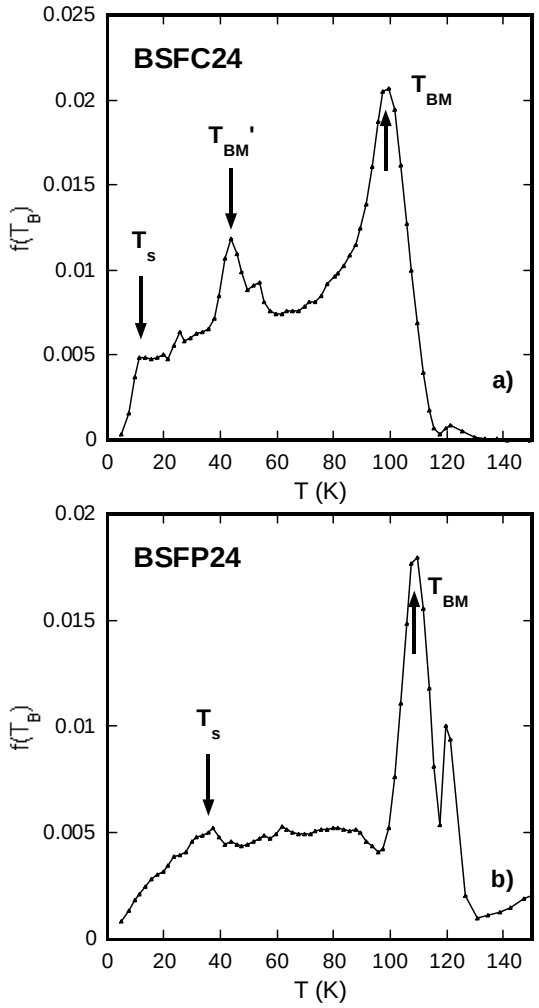

Figure 4: Temperature dependence of the distribution function $f(T_B)$ for (a) BSFC24 and (b) BSFP24.

can speculate that the ~ 100 K peak of the $f(T_B)$ corresponds likely to the blocking of the 20 nm particle macrospins. This is consistent with the ~ 100 K peaks of the BSFP17 and BSFP24 samples, which show a clear 20 nm particle presence. The 43 K peak is characteristic only to the Cr_2O_5 samples and it might be related to the rich presence of nanoparticles with intermediate sizes betwee 8-12 nm. This assumption is also based on the lack of the 43 K peak in the P_2O_5 samples and the lack of intermediate size particles in these samples, as seen in Figs 1(b) and 2(b). Finally, following the same line of observations, it is likely that the shoulder peak is due to the blocking of the smallest of the nanoparticles, of diameters below 5 nm.

We should point out that the correlation between the two types of distributions is not perfect, mainly because the blocking temperature distribution reflects the magnetic size and not the geometric size. Therefore, $f(T_B)$ shoud include extra information compared to the size distribution. Actually, SANS measurements [6] proved the existence of a magnetically-dead layer which can have an important contribution in the case of the smallest nanoentities. Nevertheless, based on the observed correlation between the two distributions, we can conclude that the low-temperature peculiarities of the ZFC magnetization *m* vs. temperature *T*, as observed in Refs. 4 and 5, are a result of the unblocking of the tiniest nanoparticles of magnetite and not other mechanisms like domain motion [7].

4 CONCLUSIONS

Here we report on the size distribution and the resulting blocking temperatures of magnetic entities grown in magnetite-based glass-ceramics obtained from borosilicate parent glasses with two different contents of Fe and two different nucleating agents. The content of iron leads to the growth of a series of submicron magnetite crystallites and to a large amount of nanoparticles with nontrivial distributions. In particular, the P_2O_5 nucleating agent leads to a clearly separated bimodal distribution. A simple analysis of the distribution of the blocking temperatures shows correlations with particle size distribution. However, this correlation is not perfect, thus hinting to a more complex magnetic structure of the nanoparticles and possibly strong inteparticle interactions.

5 ACKNOWLEDGEMENTS

This work was supported by a grant of the Romanian National Authority for Scientific Research and Innovation, CNCS/CCCDI - UEFISCDI, project number PN-III-P2-2.1-PED-2016-1741 (contract 163PED/2017), ROMBRICKS, Core Program PN 10/2016 at NIMP and by the Office of Naval Research at USNA.

6 REFERENCES

[1] N. Kreidl, J. Non-Cryst. Solids, 129, 1-11, 1991.
[2] D. Manara, A. Grandjean, DR Neuville, J. Non-Cryst Solids, 355, 2528–253, 2009.
[3] V. Sandu, M. S. Nicolescu, V. Kuncser, S. Popa, I. Pasuk, C. Ghica, E. Sandu, Journal of Nanoscience and Nanothechnology, 12 (6), 5043–5050, 2012; V. Sandu, S. Greculeasa, A. Kuncser, V. Kuncser, J. Am. Ceram. Soc, 99 (12), 4013–4021, 2016.
[4] V. Sandu, E. Cimpoiasu, S. Greculeasa, A. Kuncser, M. S. Nicolescu, Ceramics International, 43, 3405, 2017.
[5] V. Sandu, E. Cimpoiasu, A. Kuncser, M. S. Nicolescu , submitted.
[6] V.S. Raghuwanshi, R. Harizanova, S. Haas, D. Tatchev, I. Gugov, C. Dewhurst, C. Rüssel, A. Hoell, J. Non-Cryst. Solids 385, 24–29, 2014.
[7] M. Bałanda, A. Wiecheć, D. Kim, Z. Kąkol1, A. Kozłowski, P. Niedziela, J. Sabol, Z. Tarnawski1, and J.M. Honig, Eur. Phys. J. B 43, 201–212, 2005.